ABSTRACT

Title of dissertation: Search for Pair Production of Third-Generation Scalar Leptoquarks and R-Parity Violating Stops in Proton-Proton Collisions at $\sqrt{s} = 8\,\mathrm{TeV}$

Kevin Pedro, Doctor of Philosophy, 2014

Dissertation directed by: Professor Sarah C. Eno
Department of Physics

insert abstract here

Search for Pair Production of Third-Generation Scalar Leptoquarks and R-Parity Violating Stops in Proton-Proton Collisions at $\sqrt{s} = 8\,\mathrm{TeV}$

by

Kevin Pedro

Dissertation submitted to the Faculty of the Graduate School of the
University of Maryland, College Park in partial fulfillment
of the requirements for the degree of
Doctor of Philosophy
2014

Advisory Committee:
Professor Sarah C. Eno, Chair/Advisor

Dedication

To my parents, Philip and Lisa

Acknowledgments

insert acknowledgments here

Table of Contents

List of Tables

List of Figures

List of Abbreviations

ALICE	A Large Ion Collider Experiment
APD	Avalanche Photodiode
APV	Atomic Parity Violation
ATLAS	A Toroidal LHC ApparatuS
BPTX	Beam Pick-up Timing for the eXperiments
BRW	Buchmüller-Rückl-Wyler
BSM	Beyond Standard Model
CERN	European Organization for Nuclear Research
CL	Confidence Level
CMS	Compact Muon Solenoid
CMSSW	CMS Software
CP	Charge-Parity
CPU	Central Processing Unit
CSC	Cathode Strip Chamber
CTF	Combinatorial Track Finder
DAQ	Data Acquisition
DT	Drift Tube
EB	ECAL Barrel
ECAL	Electromagnetic Calorimeter
EE	ECAL Endcap
EM	Electromagnetic
FCNC	Flavor-Changing Neutral Current
FSR	Final-State Radiation
GSF	Gaussian Sum Filter
GUT	Grand Unified Theory
HB	HCAL Barrel
HCAL	Hadron Calorimeter
HE	HCAL Endcap
HEEP	High Energy Electron Pairs
HERA	Hadron-Electron Ring Accelerator
HF	HCAL Forward
HO	HCAL Outer
HPD	Hybrid Photodiode
HLT	High-Level Trigger
IP	Interaction Point
ISR	Initial-State Radiation
L1	Level 1
L1A	Level-1 Accept
LEP	Large Electron-Positron Collider

LHC	Large Hadron Collider
LHCb	Large Hadron Collider beauty
LQ	Leptoquark
LO	Leading Order
mBRW	minimal Buchmüller-Rückl-Wyler
MB	Muon Barrel
MC	Monte Carlo
ME	Muon Endcap
MET	Missing Transverse Energy
MIP	Minimum Ionizing Particle
NLO	Next-to-Leading Order
NNLO	Next-to-Next-to-Leading Order
PD	Primary Dataset
PF	Particle Flow
PDF	Parton Distribution Function
PMT	Photomultiplier Tube
PS	Proton Synchrotron, Preshower
PSB	Proton Synchrotron Booster
QED	Quantum Electrodynamics
QCD	Quantum Chromodynamics
RBX	Readout BoX
RF	Radio Frequency
RMS	Root Mean Square
RPC	Resistive Plate Chamber
RPC	R-Parity Conserving
RPV	R-Parity Violating
SiPM	Silicon Photomultiplier
SLHA	SUSY Les Houches Accord
SM	Standard Model
SPS	Super Proton Synchrotron
SUSY	Supersymmetry
TCS	Trigger Control System
TEC	Tracker End Cap
TIB	Tracker Inner Barrel
TID	Tracker Inner Disks
TOB	Tracker Outer Barrel
TPG	Trigger Primitive Generator
TTC	Timing, Trigger and Control
VPT	Vacuum Phototriode
WLS	Wavelength-Shifting

Chapter 1: Introduction

Chapter 2: Theoretical Motivations

2.0 The Standard Model

2.1 Leptoquarks

2.2 R-Parity Violating Supersymmetry

Chapter 3: Compact Muon Solenoid Experiment

3.0 The Large Hadron Collider

3.1 Tracker

3.2 Electromagnetic Calorimeter

3.3 Hadronic Calorimeter

3.4 Solenoid

3.5 Muon System

3.6 Trigger

3.7 Luminosity Measurement

Chapter 4: Event Reconstruction

4.1 Event Generation

4.2 Detector Simulation

4.3 Particle Flow

4.4 Tracks and Vertices

4.5 Electrons

4.6 Muons

4.7 Jets

4.8 b-tagging

Chapter 5: Data Analysis

5.1 Data Samples

5.1.1 Observed data

5.1.2 Monte Carlo

5.2 Selection and Optimization

5.2.1 Object Identification

5.2.2 Event Selection

5.3 Background Estimations

5.3.1 Irreducible Background (ttbar)

5.3.2 Reducible Background (fake tau)

5.3.3 Reducible Background (QCD)

5.3.4 Other Backgrounds

5.4 Systematic Uncertainties

5.5 Results

Chapter 6: Calorimeter Upgrades

6.1 Phase 1 Simulations

6.1.1 HE Radiation Damage Model

6.1.2 Jet Studies with Radiation Damage

6.2 Phase 2 Simulations

6.2.1 Validation of Upgrade Standalone Simulation

6.2.2 Tests of Physics Effects on Pion Response and Resolution

6.2.3 HE Rebuild/Extension + Shashlik ECAL Jet Studies

6.3 Hadronic Fast Simulation

6.3.1 Retuning of Hadronic Response

6.4 Double-sided Crystal Ball

PDF and CDF definitions:

$$\int_{-\infty}^{\infty} f(x)dx = 1 \tag{6.1}$$

$$F(x) = \int_{-\infty}^{x} f(x')dx' \tag{6.2}$$

Parameters:

$$\vec{p} = (\mu, \sigma, a_L, n_L, a_R, n_R) \tag{6.4}$$

$$d_L = n_L/a_L \tag{6.5}$$

$$d_R = n_R/a_R \tag{6.6}$$

Parameter conditions:

$$n_L, n_R > 1 \tag{6.7}$$

$$a_L, a_R > 0 \tag{6.8}$$

Normalization:

$$N = \frac{1}{\sigma\left[\frac{d_L}{n_L-1}\cdot\exp\left(-\frac{a_L^2}{2}\right)+\sqrt{\frac{\pi}{2}}\left(\mathrm{erf}\left(\frac{a_L}{\sqrt{2}}\right)+\mathrm{erf}\left(\frac{a_R}{\sqrt{2}}\right)\right)+\frac{d_R}{n_R-1}\cdot\exp\left(-\frac{a_R^2}{2}\right)\right]} \tag{6.9}$$

Probability density function:

$$f(x;\vec{p}) = N\cdot\begin{cases}\exp\left(-\frac{a_L^2}{2}\right)\cdot\left[\frac{1}{d_L}\left(d_L-a_L-\frac{x-\mu}{\sigma}\right)\right]^{-n_L} & \text{for } \frac{x-\mu}{\sigma}\leq -a_L\\[4em] \exp\left(-\frac{1}{2}\left(\frac{x-\mu}{\sigma}\right)^2\right) & \text{for } -a_L<\frac{x-\mu}{\sigma}<a_R\\[4em] \exp\left(-\frac{a_R^2}{2}\right)\cdot\left[\frac{1}{d_R}\left(d_R-a_R+\frac{x-\mu}{\sigma}\right)\right]^{-n_R} & \text{for } \frac{x-\mu}{\sigma}\geq a_R\end{cases} \tag{6.10}$$

Cumulative distribution function:

$$
F(x;\vec{p}) = \sigma N \cdot \begin{cases}
\frac{d_L}{n_L-1}\exp\left(-\frac{a_L^2}{2}\right)\left[\frac{1}{d_L}\left(d_L - a_L - \frac{x-\mu}{\sigma}\right)\right]^{-n_L+1} & \text{for } \frac{x-\mu}{\sigma} \leq -a_L \\
\\
\frac{d_L}{n_L-1}\exp\left(-\frac{a_L^2}{2}\right) + \sqrt{\frac{\pi}{2}}\mathrm{erf}\left(\frac{a_L}{\sqrt{2}}\right) + \sqrt{\frac{\pi}{2}}\mathrm{erf}\left(\frac{x-\mu}{\sigma\sqrt{2}}\right) & \text{for } -a_L < \frac{x-\mu}{\sigma} < a_R \\
\\
\frac{d_L}{n_L-1}\exp\left(-\frac{a_L^2}{2}\right) + \sqrt{\frac{\pi}{2}}\mathrm{erf}\left(\frac{a_L}{\sqrt{2}}\right) & \\
+\sqrt{\frac{\pi}{2}}\mathrm{erf}\left(\frac{a_R}{\sqrt{2}}\right) + \frac{d_R}{n_R-1}\exp\left(-\frac{a_R^2}{2}\right) & \\
+\frac{d_R}{1-n_R}\exp\left(-\frac{a_R^2}{2}\right)\left[\frac{1}{d_R}\left(d_R - a_R + \frac{x-\mu}{\sigma}\right)\right]^{-n_R+1} & \text{for } \frac{x-\mu}{\sigma} \geq a_R
\end{cases} \tag{6.11}
$$

$$
= \sigma N \cdot \begin{cases}
B_L\left[\frac{1}{d_L}\left(d_L - a_L - \frac{x-\mu}{\sigma}\right)\right]^{-n_L+1} & \text{for } \frac{x-\mu}{\sigma} \leq -a_L \\
\\
A_L + C_L + \sqrt{\frac{\pi}{2}}\left(1 - \mathrm{erfc}\left(\frac{x-\mu}{\sigma\sqrt{2}}\right)\right) & \text{for } -a_L < \frac{x-\mu}{\sigma} < a_R \\
\\
A_L + C_L + C_R + A_R & \\
+B_R\left[\frac{1}{d_R}\left(d_R - a_R + \frac{x-\mu}{\sigma}\right)\right]^{-n_R+1} & \text{for } \frac{x-\mu}{\sigma} \geq a_R
\end{cases} \tag{6.12}
$$

Inverse cumulative distribution function:

$$x = \begin{cases} \mu + \sigma \left(-d_L \left[\frac{y}{\sigma N} / B_L \right]^{\frac{1}{-n_L+1}} - a_L + d_L \right) & \text{for } y < \sigma N A_L \\ \\ \mu + \sigma \sqrt{2} \text{erfc}^{-1} \left[1 - \sqrt{\frac{2}{\pi}} \left(\frac{y}{\sigma N} - A_L - C_L \right) \right] & \text{for } \sigma N A_L \leq y \leq \sigma N (A_L + C_L + C_R) \\ \\ \mu + \sigma \left(d_R \left[\frac{\frac{y}{\sigma N} - A_L - C_L - C_R - A_R}{B_R} \right]^{\frac{1}{-n_R+1}} + a_R - d_R \right) & \text{for } y > \sigma N (A_L + C_L + C_R) \end{cases} \tag{6.13}$$

6.4.1 MIP Fraction in Hadronic Showers

In the CMS hadronic shower fast simulation, the shower starting depth s is simulated using an exponential distribution. Integrate to find the cumulative distribution for inversion sampling, where $x \in [0, 1]$ is a uniformly distributed random number:

$$f(s) = e^{-s} \tag{6.14}$$

$$F(s) = \int_0^s f(s')ds' = 1 - e^{-s} \tag{6.15}$$

$$x \equiv F(s) \to F^{-1}(x) = -\ln(1 - x) = \ln\left(\frac{1}{x}\right) = s \tag{6.16}$$

In the last step, the fact that x is a uniformly distributed random number in $[0, 1]$ is used to take $(1 - x) \to x$.

The condition which decides if the shower will start in ECAL is based on a comparison between the depth of ECAL d_{ecal} and the starting depth s. If the shower does not start in ECAL, the incident hadron is considered to be a MIP (minimum ionizing particle) in ECAL.

$$\frac{d_{\text{ecal}} - s}{d_{\text{ecal}}} > 0.1 \tag{6.17}$$

$$\rightarrow 0.9 d_{\text{ecal}} > s (\text{for pion showers starting in ECAL}) \tag{6.18}$$

$$\rightarrow 0.9 d_{\text{ecal}} \leq s (\text{for pions which are MIPs in ECAL}) \tag{6.19}$$

$$\rightarrow d \equiv 0.9 d_{\text{ecal}} (\text{the minimum starting distance for MIPs}) \tag{6.20}$$

Since $f(s)$ is a probability distribution, it has area 1 in $[0, \infty]$. The area for $s = d..\infty$, i.e. when $s \geq d$, should be equal to the probability p that the particle is a MIP. In order to solve this problem, the distribution must be transformed to introduce a free parameter:

$$f(s, \lambda) = \lambda e^{-\lambda s} \tag{6.21}$$

$$s = \frac{1}{\lambda} \ln \left(\frac{1}{x} \right) \tag{6.22}$$

Now the integral can be solved to require the correct MIP fraction:

$$p = \int_d^\infty ds \lambda e^{-\lambda s} = e^{-\lambda d} \tag{6.23}$$

$$\rightarrow \lambda = \frac{1}{d} \ln \left(\frac{1}{p} \right) \tag{6.24}$$

Since d is determined by detector geometry, for any $p \in (0, 1)$, λ can be found to ensure the correct MIP fraction. The final result is just a scaling by $1/\lambda$ of the original equation for randomly generating s from the uniform random number x. In practice, p can be determined from full simulation as a function of incident particle energy and η. The easiest way to do this would be to store values for each η and the same energy points that are used in HCALResponse, and then interpolate for intermediate energies. (See Figures 6.1 and 6.2 for examples.) For energies outside that range, the first or last values should be used rather than extrapolating, since extrapolating could produce $p \leq 0$ or $p \geq 1$, which would create unphysical values of λ, i.e. $\lambda \notin (0, \infty)$.

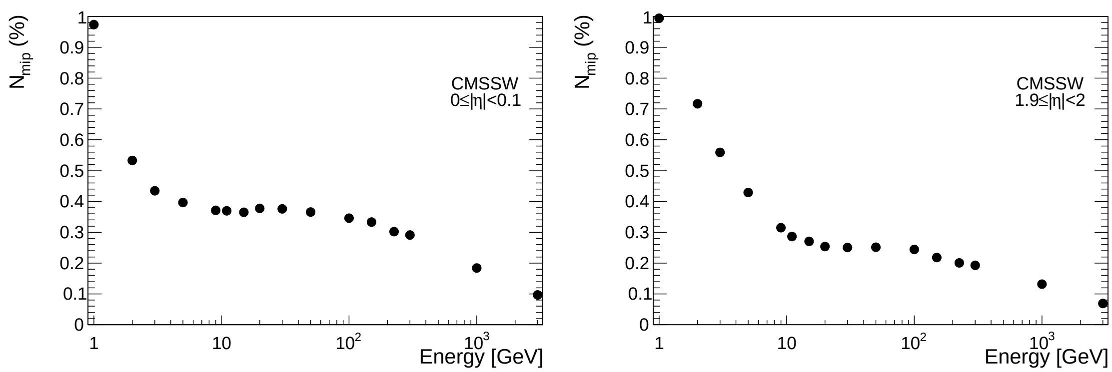

Figure 6.1: Plots of MIP percentage vs. energy for $i\eta = 1$ (in the barrel) and $i\eta = 20$ (in the endcap).

6.5 Dose Rate Effects

6.5.1 Dose Rate Effect Models

6.5.2 Scintillator Radiation Damage Studies

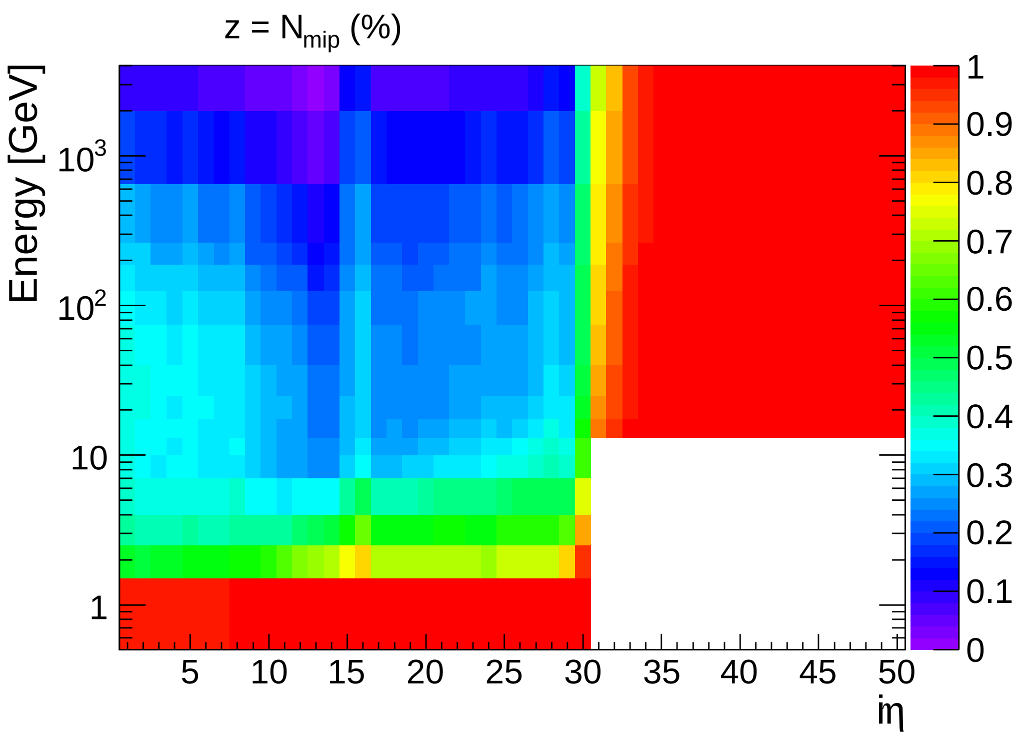

Figure 6.2: Plots of MIP percentage vs. energy and η for the entire calorimeter system.

Chapter 7: Conclusions

Chapter A: Full CLs Shape-Based Limits

Chapter B: Event Displays

Chapter C: Table of Monte Carlo Datasets

Chapter D: CMS Collaboration